

# Metal ion release from nitrogen ion implanted CoCrMo orthopedic implant material

Orhan Öztürk<sup>a,\*</sup>, Uğur Türkan<sup>b</sup>, Ahmet E. Eroğlu<sup>c</sup>

<sup>a</sup> Department of Physics, Izmir Institute of Technology, Urla 35430, Izmir, Turkey

<sup>b</sup> Materials Science and Engineering Program, Izmir Institute of Technology, Urla 35430, Izmir, Turkey

<sup>c</sup> Chemistry Department, Izmir Institute of Technology, Urla 35430, Izmir, Turkey

Received 17 May 2005; accepted in revised form 8 August 2005

Available online 24 October 2005

## Abstract

CoCrMo alloys are used as orthopedic implant materials because of their excellent mechanical and corrosion properties. However, when placed in vivo, these alloys release Co, Cr, Mo ions to host tissues, which may give rise to significant health concerns over time. Nitrogen ion implantation can be used to form protective layers on the surface of CoCrMo orthopedic alloys by modifying the near surface layers of these materials. In this study, medical grade CoCrMo alloy (ISO 5832-12) was ion implanted with 60 keV nitrogen ions to a high dose of  $1.9 \times 10^{18}$  ions/cm<sup>2</sup> at substrate temperatures of 100, 200 and 400 °C. The N implanted layer microstructures, implanted layer phases, and thicknesses were studied by a combination of Bragg–Brentano ( $\theta/2\theta$ ) and grazing incidence (Seeman–Bohlin) X-ray diffraction (XRD and GIXRD) and cross-sectional scanning electron microscopy (SEM). Atomic force microscopy (AFM) was used for roughness analysis of N implanted as well as as-polished surfaces. Static immersion tests were performed to investigate metal ion release into simulated body fluid (SBF) by electrothermal atomic absorption spectrometry (ETAAS) and inductively coupled plasma optical emission spectrometry (ICP-OES). XRD and SEM analyses indicated that the N implanted layers were ~150–450 nm thick and composed of the (Co,Cr,Mo)<sub>2+x</sub>N nitride phase and a high N concentration Co-based FCC phase,  $\gamma_N$  depending on the substrate temperature. ETAAS analysis results showed that in vitro exposure of the N implanted surfaces resulted in higher levels of cobalt ion release into the simulated body fluid compared to the untreated, polished alloy. The higher Co release from the N implanted specimens is attributed to the nature of the implanted layer phases as well as to the rougher surfaces associated with the N implanted specimens compared to the relatively smooth surface of the untreated material. SEM analysis of N implanted and untreated specimens after immersion tests clearly indicated calcium phosphate formation on the as-polished CoCrMo alloy, indicating a degree of bioactivity of the untreated metal surface which is absent in the N implanted specimens.

© 2005 Elsevier B.V. All rights reserved.

**Keywords:** Cobalt–chromium–molybdenum alloy; Metal ion release; Nitrogen ion implantation; Simulated body fluid; X-ray diffraction; Atomic absorption spectroscopy; Atomic force microscopy

## 1. Introduction

CoCrMo alloys are considered to be biocompatible materials and are used widely for orthopedic applications such as hip and knee joint replacements [1–3]. The biocompatibility of CoCrMo alloy is related closely to this material's excellent corrosion resistance, imparted by a thin passive oxide film that forms spontaneously on the alloy surface. X-ray photoelectron spectroscopy (XPS) analysis reveals that its composition is predominantly Cr<sub>2</sub>O<sub>3</sub> oxide with some minor contributions from

Co and Mo oxides [4]. Such films also form on the surfaces of other metallic biomaterials (e.g., stainless steels, titanium and its alloys) and serve as a barrier to corrosion processes in alloy systems that would otherwise experience high corrosion rates.

Once implanted and exposed to the aggressive body environment (biological fluids in the body contain water, salt, dissolved oxygen, bacteria, proteins, and various ions such as chloride and hydroxide), CoCrMo alloys tend to corrode over time, releasing Co, Cr, Mo ions into body fluids (serum, urine, etc.). Implant components fabricated from CoCr-based alloys have been reported to produce elevated Co, Cr, and Ni concentrations in body fluids. Over time the level of metal ions may become clinically significant resulting in implant failure,

\* Corresponding author. Tel.: +90 232 750 7513; fax: +90 232 750 7509.

E-mail address: [orhanozturk@iyte.edu.tr](mailto:orhanozturk@iyte.edu.tr) (O. Öztürk).

osteolysis, and allergic reactions. The toxic effects of metals (Ni, Co, Cr, Al and V) released from orthopedic implants are well documented [5]. A recent study investigating the corrosion products of CoCrMo and 316L alloys found CoCrMo corrosion products to be more toxic than those of 316L. The most toxic ions were Cr, Ni, and Co [6].

Metallic ions from orthopedic implant materials are released into the body environments by the processes of electrochemical corrosion or chemical dissolution, wear, and mechanically accelerated electrochemical processes such as corrosion fatigue and fretting corrosion. Research shows that the corrosion of CoCr alloys in neutral or acid solutions takes place primarily by selective dissolution of cobalt. The oxide film on CoCrMo alloy inhibits the dissolution of metal ions but is not always stable in the human body. Hanawa et al. [7] characterized the surface oxide films formed on CoCrMo alloy during immersion in various simulated biological environments, Hank's solution, cell culture medium and incubation with cultured cells. Cobalt was dissolved during immersion in Hank's solution, cell culture media and by incubation in cell culture; after dissolution, the surface film consisted of chromium oxide containing a small amount of molybdenum oxide. The oxide film thickness may also be a factor in metal ion release since the oxide films present on the surface of CoCrMo alloy are extremely thin ( $\sim 1\text{--}4$  nm) and therefore susceptible to fracture due to scratches, dents and wear. Oxide fracture in aqueous environments produces oxide particles and exposes the reactive base alloy to water resulting in the dissolution of base alloy (producing metal ions) [8].

There are various surface treatment methods which may prevent and/or reduce the release of potentially harmful metal ions from orthopedic implant materials. One is to thicken the protective oxide layer already present on the surface of metallic biomaterials via a process known as passivation (commercially available chemical treatment with hot, concentrated nitric acid). A recent study [4] investigating the surface passive films on CoCrMo alloy in simulated physiological solution found that passivation decreased the apparent cobalt content of the surface by increasing the thickness of the chromium-rich oxide layer. Another method is to apply coatings or protective layers, to act as a physical barrier between the aggressive body environment and the biomaterial to be protected. Quite a few literature studies related to various types of coatings such as TiN and ZrO<sub>2</sub> on CoCrMo and Ti6Al4V show that these coatings are better barriers to ionic diffusion than are the native surface oxides [8–10].

In the present study, we examine nitrogen ion implantation as a means to form protective layers on the surface of CoCrMo alloys and investigate the effectiveness of nitrogen implanted layers in preventing metal ion release from CoCrMo orthopedic materials. It is generally accepted that nitrogen ion implantation is an excellent method to enhance the wear and corrosion resistance of a wide range of materials [11,12]. Several researchers have utilized ion beam techniques in the medical area [13,14], such as for orthopedic prostheses that require high wear resistance and excellent corrosion properties as well as biocompatibility. Cui and Luo [13] reported a significant reduction in polyethylene wear for the nitrogen ion implanted

cobalt–chromium femoral head. (Most artificial joints consist of a metallic component articulating against a polymer. The metallic component is mainly made from either CoCr alloys or titanium/titanium alloy while the polymer component is mainly ultrahigh molecular weight polyethylene. The main problem existing in such artificial joints is prosthetic wear debris generated from the polymeric 'cup' which is believed to be a major cause of aseptic loosening [13].)

In a recent study [15], an ion implantation technique, namely Plasma Based Ion Implantation, which can facilitate three dimensional ion implantation by plasma processes, was used to improve the wear and corrosion resistances of Co–Cr femoral heads. This study found that the wear resistance of Co–Cr alloy with a high nitrogen ion implantation dose was superior to the untreated Co–Cr alloy and the process of N implantation was effective in enhancing corrosion resistance of the Co–Cr alloy. In another investigation [16], orthopedic materials (CoCrMo and Ti–6Al–4V) were nitrided at temperatures up to 850 °C by an ion implantation process known as high intensity plasma ion nitriding (low energy ion implantation at elevated temperatures). This study (via XRD and SEM) concluded that the enhanced wear properties of the CoCrMo alloys could be attributed to the formation of thick nitrogen implanted layers and to the formation of specific microstructures at the surface.

A literature survey reveals no studies related directly to metal ion release from nitrogen ion implanted orthopedic alloys. The purpose of this study is therefore to investigate metal ion release from nitrogen ion implanted CoCrMo orthopedic alloy materials and the effectiveness of nitrogen implanted layers in preventing and/or reducing the dissolution of metal ions into the body fluids. Our study combines the use of X-ray diffraction (XRD) and cross-sectional scanning electron microscopy (SEM). Metal ion release into simulated body fluid (SBF) is investigated via atomic absorption spectroscopy (AAS) and inductively coupled plasma optical emission spectroscopy (ICP-OES).

## 2. Experimental materials and methods

### 2.1. Materials: CoCrMo alloy

Medical grade cobalt–chromium–molybdenum (CoCrMo) alloy (ISO 5832-12) with a base chemical composition of 26% Cr, 6% Mo and balance Co (all in wt.%), was the material into which nitrogen was implanted. The specimens had a disc-like geometry with a diameter of 3.0 cm and a thickness of 0.30 cm. The grain size for the specimens of this study, obtained by metallography, was  $\sim 5$  to 15  $\mu\text{m}$ . Before implantation, all the specimens were polished to mirror-like quality with a mean surface roughness (Ra) of about 1.78 nm based on atomic force microscopy (AFM).

### 2.2. Nitrogen ion implantation

Nitrogen ion implantation was carried out with a relatively simple, broad beam (beam size up to  $\sim 10$  cm in diameter), ultrahigh current density ion implanter. A detailed description of

the essential elements of this type of system can be found elsewhere [17]. The N ions generated by the implantation system were not mass analyzed, but primarily consist of  $N_2^+$  (~70%) and  $N^+$  (~30%). The polished CoCrMo alloy specimens were ion implanted with 60 keV nitrogen ions to a high dose of  $1.9 \times 10^{18}$  N/cm<sup>2</sup> at substrate temperatures of 100, 200 and 400 °C. The N ion implantation conditions for the specimens of this research are summarized in Table 1. The temperatures of the CoCrMo specimens during N implantation were measured by a thermocouple attached to the back of the samples. The specimens were heated by the ion beam. A constant processing temperature for a given specimen was assured principally by control of the ion beam. Additional temperature control was provided by a copper fixture through which water or liquid nitrogen can be circulated and on which the sample is clamped. More details can be found in [18]. Duplicate specimen numbers are listed and used for the various characterization techniques.

### 2.3. Characterization techniques

Near surface crystal structures, implanted layer phases, nitrogen implanted layer thicknesses and implanted layer surface roughness were characterized by X-ray diffraction (XRD), scanning electron microscopy (SEM) and atomic force microscopy (AFM). XRD was done in both the symmetric  $\theta/2\theta$  Bragg–Brentano and grazing-incidence (GIXRD) modes using a Philips X'pert XRD system in a step-scanning mode (0.05° step size and 4 s count-time per step) with Cu-K $\alpha$  radiation ( $\lambda = 1.5404$  Å for the 8.05 keV X-rays). Mean roughness Ra was measured by AFM (Nanoscope IV) for both polished (unimplanted) and N implanted CoCrMo surfaces; the equipment was operated in contact mode in air. At least three readings were taken for each surface tested. Cross-sectional SEM was performed on a few selected specimens to examine the possible use of this method for measuring the N implanted layer thicknesses. Planar-view SEM was also used for surface morphology analysis for both the unimplanted alloy and N implanted specimens. Before cross-sectional SEM analysis, specimens were polished (down to 0.05  $\mu$ m alumina), and etched electrolytically for 30 s. The type of chemical etchant was chosen such that it would preferentially etch the substrate rather than the implanted layer, and was a mixture of HCl (5 mL) and H<sub>2</sub>O<sub>2</sub> (100 mL). This etchant was also used to reveal the grain structure of the substrate alloy. Before placing the

specimens into the SEM unit, they were cleaned ultrasonically in ethyl alcohol.

### 2.4. Static immersion test

Static immersion tests were performed with both polished (unimplanted) and N implanted specimens. Immersion tests were conducted at 37 °C using simulated body fluid (SBF) containing NaCl, 6.547 g/l; NaHCO<sub>3</sub>, 2.268 g/l; KCl, 0.372 g/l; Na<sub>2</sub>HPO<sub>4</sub>, 0.124 g/l; MgCl<sub>2</sub>·H<sub>2</sub>O, 0.305 g/l; CaCl<sub>2</sub>·2H<sub>2</sub>O, 0.368 g/l; Na<sub>2</sub>SO<sub>4</sub>, 0.071 g/l. The SBF was buffered at physiological pH 7.4 at 37 °C with 50 mM trishydroxymethyl aminomethane [(CH<sub>2</sub>OH)<sub>3</sub>CNH<sub>2</sub>] and 36.23 mM HCl acid. In addition, sodium azide (NaN<sub>3</sub>, 1 g) was added into the SBF for preventing microbial effects. Before the immersion of the test specimens into the SBF, the unimplanted areas were coated with epoxy resin so that metal ion release would be detected from the N implanted regions only. To check the efficiency of the epoxy, an unimplanted (as-polished) sample was completely coated with it, and then was immersed into the SBF. The areas that were exposed to the body fluid were estimated to be 1.65 cm<sup>2</sup> and 16.0 cm<sup>2</sup> for the N implanted and the as-polished immersion test specimens, respectively. A total of 10 test specimens were involved in the immersion test: six nitrogen implanted test specimens (two for each implantation temperature; these were labeled as parallel 1 and parallel 2), two untreated specimens, and two epoxy coated untreated samples. All the test specimens were incubated in SBF at 37 °C. After immersion, the 5 mL samples were removed from incubation bottles (each containing 130 mL immersion test solution and a test specimen) to be analyzed for metal ion release periodically (after 1, 3, 7, 15 and 30 days immersion and after every month thereafter). The static immersion test duration was ~150 days.

The concentrations of metal ions released into the simulated body fluid from the untreated and N implanted test specimens were determined in ppb ( $\mu$ g/L) by electrothermal atomic absorption spectrometry (ETAAS) and inductively coupled plasma optical emission spectrometry (ICP-OES). Three readings were taken to obtain the average values of the metal ion release. A Thermo Elemental Solaar M6 series atomic absorption spectrometer was employed in the determination of Co, Cr and Ni, while Mo ion release into the SBF was monitored by ICP-OES using a Varian Liberty Series II optical emission spectrometer. For ETAAS and ICP-OES analyses, single element standard solutions (Merck Inc. 1000 mg/L) were diluted for use as the Co, Cr, Mo and Ni intermediate standard solution (1 mg/L). The matrix-matched calibration curves were established from at least five plotted points. The analytical detection limits for Co, Cr and Ni was found to be 0.5  $\mu$ g/L, while the detection limit for Mo was 20  $\mu$ g/L.

During the immersion test, the pH value of the solution was also monitored and found to vary between 7.4 and 7.6. After the static immersion test, the test specimens were visually inspected and their surface morphology and elemental analysis were studied by SEM equipped with energy dispersive X-ray spectrometry (EDX). Before the SEM/EDX analysis, the test

Table 1  
Nitrogen ion implantation conditions

Specimen no.	Temperature (°C)	Dose (ions/cm <sup>2</sup> )	Time (min)	Ra (nm)
<i>Polished substrate</i>				
S29, S34, S35	100	$1.9 \times 10^{18}$	30	5.8
S28, S32, S33	200	$1.9 \times 10^{18}$	30	12.1
S30, S31	400	$1.9 \times 10^{18}$	30	8.2

The polished CoCrMo alloy specimens were ion implanted with 60 keV nitrogen ions. Mean roughness Ra was measured by AFM for both untreated (polished) and N implanted CoCrMo surfaces.

specimens were removed from the solution, gently rinsed with distilled water and dried at room temperature.

### 3. XRD results and discussion

Fig. 1 shows the  $\theta/2\theta$  XRD (Bragg–Brentano geometry) results for the N implanted specimens at increasing substrate temperatures of 100, 200, and 400 °C. Included in the same figure are the results for the polished, untreated sample. In this XRD geometry, the effective depths probed by Cu-K $\alpha$  X-ray beams were obtained from  $\sin\theta/2\mu$  [19] ( $\mu$  is the linear mass absorption coefficient, estimated to be  $2540\text{ cm}^{-1}$  for this CoCrMo alloy) to be 0.51 and  $1.50\text{ }\mu\text{m}$  for  $2\theta$  scan angles between  $30^\circ$  and  $100^\circ$ , respectively. In Fig. 1, the substrate (CoCrMo) peaks are labeled as “ $\gamma$ (hkl)” for the fcc  $\gamma$ -(Co,Cr,Mo) phase and “ $\epsilon$ -(hkl)” for the hcp  $\epsilon$ -(Co,Cr,Mo). The volume

percent of the substrate  $\gamma$  phase is estimated to be about 90%, while the rest (10%) is due to the substrate  $\epsilon$  phase.

An important observation from Fig. 1 is the formation of an interstitial phase (nitrogen occupying octahedral sites in fcc lattice) labeled as  $\gamma_N$  for the specimen implanted at 400 °C. The  $\gamma_N$  phase formation is similar to that observed for nitrogen implantation of 304 stainless steel at 400 °C where  $\gamma_N$  forms from the  $\gamma$ -(Fe,Cr,Ni) parent structure [17]. Note that the parent structure of the substrate material in this study is  $\gamma$ -(Co,Cr,Mo). Based on Ref. [17], the  $\gamma_N$  phase was observed when the substrate temperature was held near 400 °C. The  $\gamma_N$  phase is known to be metastable. The metastability is associated with the fact that at lower and higher implantation temperatures the  $\gamma_N$  is not produced. Higher implantation temperatures ( $>500\text{ }^\circ\text{C}$ ) lead to the dissolution of the Cr resulting in a phase separated mixture of bcc-FeNi and CrN, while lower implantation

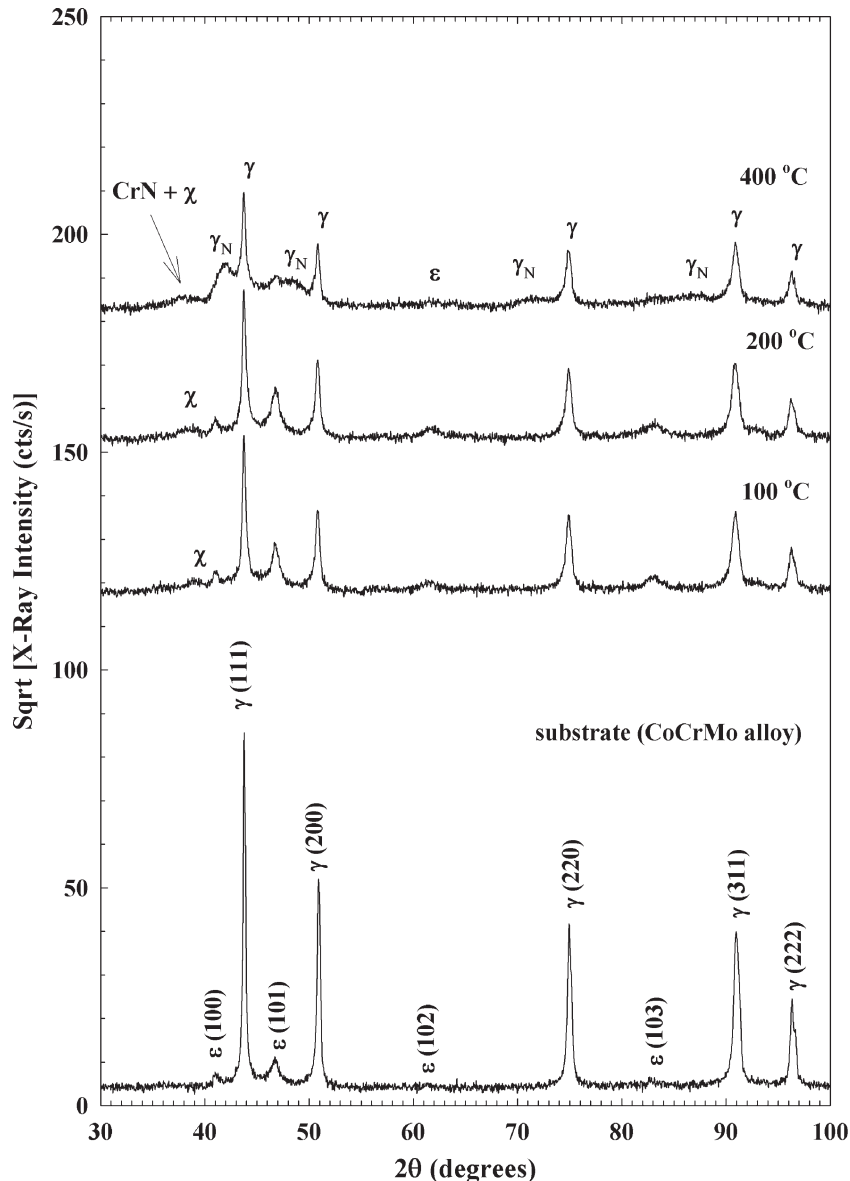


Fig. 1. XRD data for the unimplanted CoCrMo alloy specimen (the substrate material) and the specimens nitrogen implanted at substrate temperatures of 100, 200, and 400 °C. The use of the square root intensity is to visually enhance the weaker peaks.

temperatures ( $\sim 200$  to  $350$  °C) result in a hexagonal nitride phase,  $\epsilon$ -(Fe,Cr,Ni) $_{2+x}$ N [17].

The XRD results for the specimens implanted at  $100$  and  $200$  °C show a peak labeled “ $\chi$ ” for the (Co,Cr,Mo) $_{2+x}$ N phase. The XRD peaks associated with this phase are weak (low intensity) and broad suggesting a distribution of nitrogen in a very thin implanted layer (about  $100$  nm or less based on the cross-sectional SEM results to be discussed later). This peak is shifted to lower angles as the implantation temperature increases. The (Co,Cr,Mo) $_{2+x}$ N phase is referred to as the hexagonal nitride phase and is quite similar to the epsilon nitride phase (Fe,Cr,Ni) $_{2+x}$ N, which forms in the surface layers of nitrogen implanted 304 SS [17].

To reveal the N implanted layer phases at the near surface, grazing incidence X-ray diffraction (GIXRD) of the same specimens in Fig. 1 was carried out at the incident angles of  $\omega=0.5^\circ$  and  $1^\circ$  and the results are shown in Fig. 2. In this case

(Seeman–Bohlin geometry), the effective depths probed by Cu-K $\alpha$  X-ray beams at these incident angles were estimated from  $\sin\omega/\mu$  [19] to be about  $34$  and  $68$  nm, respectively. (Note that Seeman–Bohlin geometry facilitates diffraction from crystal grains not parallel to the surface, while in Bragg–Brentano geometry the diffracted X-rays from grains oriented parallel to the surface are detected.) The GIXRD scans at the incident angle ( $0.5^\circ$ ) indicate that the top N implanted layer ( $\sim 30$  nm) for the specimens implanted at  $100$  and  $200$  °C substrate temperatures is mainly composed of the (Co,Cr,Mo) $_{2+x}$ N nitride phase. The GIXRD results at higher incident angle ( $1^\circ$ ) show more contribution coming from the substrate phase due to the increased penetration depth at this angle.

The XRD results in Fig. 1 for the specimen implanted at  $400$  °C show a peak labeled as “CrN+ $\chi$ ”. This peak is revealed much more clearly at grazing incident angle geometry and is believed to be mainly due to the (Co,Cr,Mo) $_{2+x}$ N nitride phase,

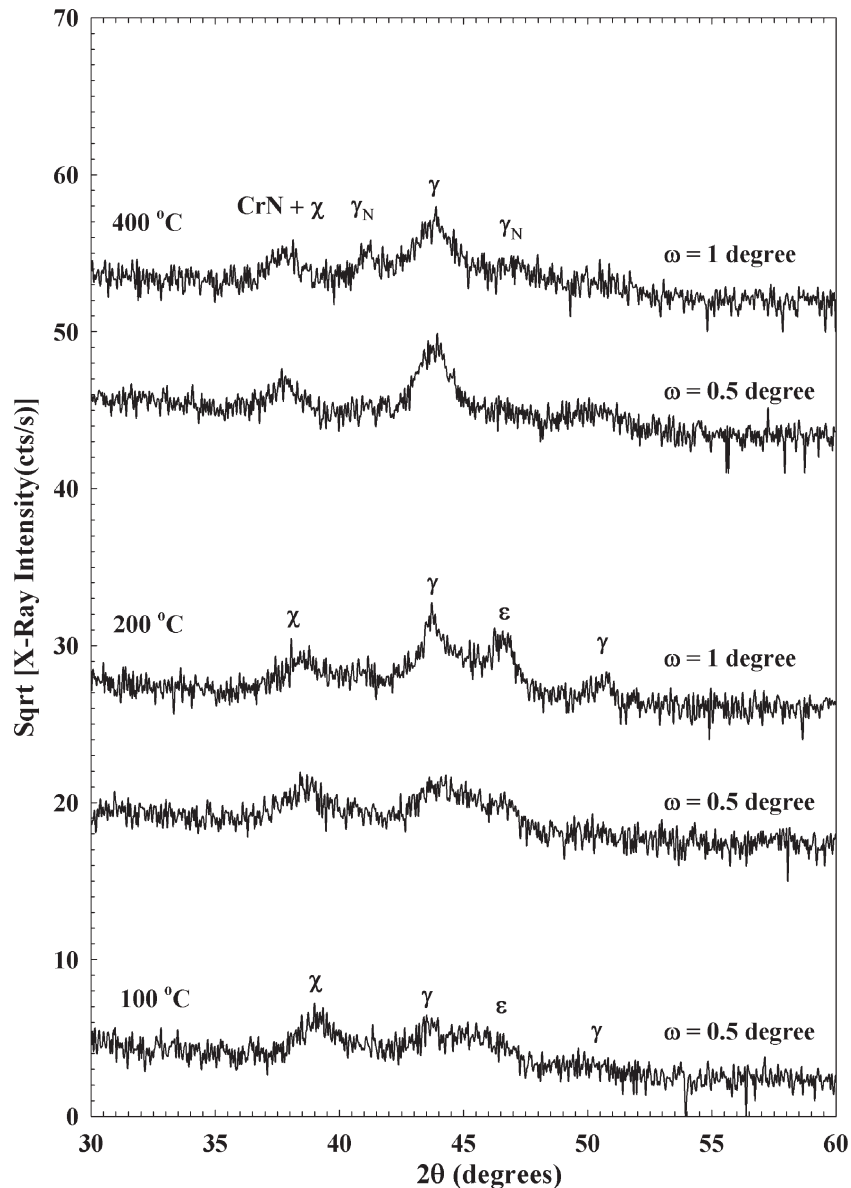


Fig. 2. GIXRD data for the specimens nitrogen implanted at substrate temperatures of  $100$ ,  $200$ , and  $400$  °C.

however, there may be a CrN component [JCPDS database (#76-1494)] to it. There may be some CrN on the top implanted surface but it is probably located in such a thin implanted layer that it is not possible to detect it via GIXRD. The small intensity and broadness of this peak suggest that this layer is very thin ( $\sim 20$  nm). Some evidence of CrN formation was presented by a research study [20] which (via GIXRD and XPS) investigated plasma immersion ion implantation (PI<sup>3</sup>) of 316 SS [an (Fe,Cr,Ni) stainless steel] at 400 °C. The GIXRD data showed the formation of the expanded austenite phase,  $\gamma_N$  in the implanted layer. The XPS analysis of the first 20 nm of the PI<sup>3</sup> treated layer showed that CrN and Cr<sub>2</sub>O<sub>3</sub> phases were distributed in the first 18 nm of the N implanted layer.

#### 4. Cross-sectional SEM analysis

Cross-sectional SEM analysis was done on the untreated substrate material and the nitrogen implanted specimens. Figs. 3 and 4 show the SEM results for the N implanted specimens at the implantation temperatures of 100, 200, and 400 °C. The SEM photomicrographs for the samples implanted at 100 and 200 °C implantation conditions clearly reveal N implanted layers with a relatively uniform thickness. The N implanted layer thicknesses obtained from the pictures in Fig. 3 are about 150 and 200 nm for the specimens implanted at 100 and 200 °C,

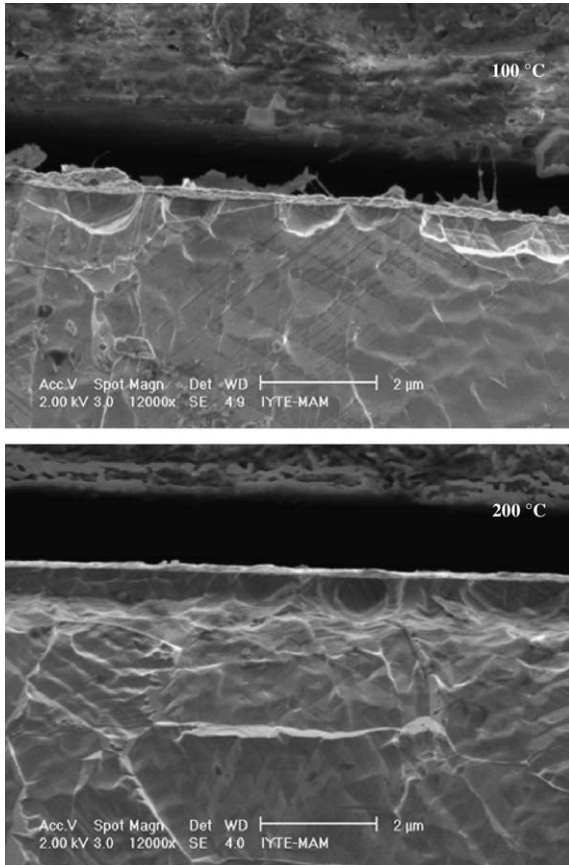


Fig. 3. Cross-sectional SEM photomicrographs for the specimens nitrogen implanted at substrate temperatures of 100 and 200 °C.

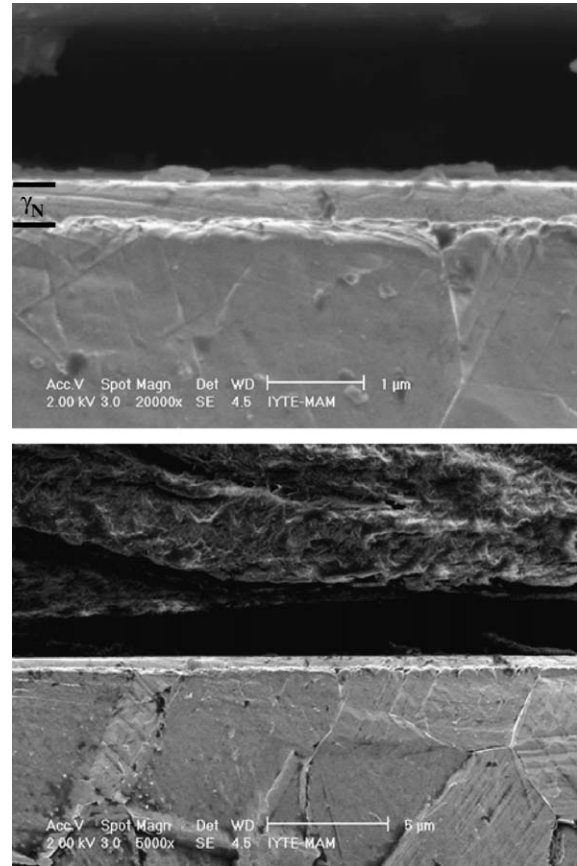


Fig. 4. Cross-sectional SEM photomicrographs for the specimen nitrogen implanted at 400 °C. These two images refer to the same region but the lower photo with higher magnification.

respectively. The photomicrographs for these samples represent two of several pictures taken along the N implanted layer. These pictures were taken sequentially over a span of several grains to look for N implanted layer thickness variations. So, based on several photomicrographs, the average layer thickness values for the 100 and 200 °C specimens are found to be 160 nm and 185 nm, respectively. Note that, based on the XRD data, the (Co,Cr,Mo)<sub>2+x</sub>N nitride phase is distributed in these thin N implanted layers.

Fig. 4 shows the SEM results for the alloy specimen N implanted at 400 °C. Both photomicrographs quite clearly reveal the extremely uniform nature of the N implanted layer, which is mainly composed of the  $\gamma_N$  phase based on the XRD results. The  $\gamma_N$  layer thickness obtained from the upper photomicrograph in Fig. 4 is about 400 nm. The average N implanted layer thickness ( $\gamma_N$  layer thickness) for this sample (based on several photomicrographs) is found to be 450 nm. An important observation related to the photomicrographs in Fig. 4 is that these pictures reveal the grain structure of the underlying substrate phase and show that the chemical etch used strongly attacks the substrate phase ( $\gamma$ ), while the  $\gamma_N$  phase is almost unaffected by the same etch. This suggests that the  $\gamma_N$  implanted layer ( $\gamma_N$  layer) may be more resistant to etching than the substrate, indicating enhanced corrosion protection of CoCrMo alloy below this surface layer.

Table 2

Nitrogen ion implanted layer thicknesses and implanted layer phases based on SEM and XRD results

Ion energy (keV)	Temperature (°C)	$L_{SEM}$ (nm)	N implanted layer phases
60	100	160	(Co,Cr,Mo) $_{2+x}$ N
60	200	185	(Co,Cr,Mo) $_{2+x}$ N
60	400	450	$\gamma_N$ , (Co,Cr,Mo) $_{2+x}$ N, CrN

The average layer thicknesses for the N implanted specimens determined by the cross-sectional SEM analysis is given in Table 2. Also included in this table are the XRD-determined N implanted layer phases.

## 5. Static immersion test results

### 5.1. Nitrogen implanted specimens

The concentration of Co ions released into the simulated body fluid from the specimens that were N implanted at 100, 200, and 400 °C were determined using ETAAS and are shown in Fig. 5. For the test specimens implanted at 100 °C, the Co ion release versus time has a steep initial rise followed by a slow increase and then it nearly becomes constant. The Co ion release behavior is quite similar for both parallel 1 and parallel 2 specimens although the amount of the Co released from the latter specimen is lower (note that the parallel 1 and parallel 2 specimens refer to the two test pieces cut from the same disk specimen that was nitrogen implanted at 100 °C). The difference between the two runs might be due to the analytical error associated with the AAS apparatus.

The ETAAS results for the Co ions released into the SBF from the specimen implanted at 200 °C show release behavior quite similar to that of the specimen implanted at 100 °C. However, the Co ion release levels are higher for the specimen implanted at 200 °C. This difference is mainly attributed to the different surface roughness values for these specimens. Based on the AFM results in Table 1, the surface roughness value for the specimen implanted at 200 °C is  $\sim 12$  nm, while it is  $\sim 6$  nm for the sample implanted at 100 °C. As discussed below, a rougher surface exposes a larger surface area for metal ion release compared to a smoother one. We cannot rule out that the difference may be due to the analytical error associated with the ETAAS experiment.

Also shown in Fig. 5 is the cobalt release behavior with the immersion time for the specimen implanted at 400 °C. The AAS results indicate quite a steep Co release for the first few time intervals ( $\sim 7$  days) of the total immersion time ( $\sim 150$  days). In addition, the Co ion release levels are higher by a factor of 2 to 3 for the specimen implanted at 400 °C compared to the specimens implanted at 100 and 200 °C substrate temperatures. As discussed below, the higher Co release levels from the specimen implanted at 400 °C might be attributed to the implanted layer phase, which, based on the XRD and SEM data, was the nitrogen solid solution phase or  $\gamma_N$ , distributed in a 450 nm thick implanted layer.

The ETAAS results for the as-polished (unimplanted) CoCrMo substrate material are also shown in Fig. 5 and indicate

reduced levels of Co ion release compared with the N implanted specimens at 100, 200 and 400 °C. The results also show that the Co ion dissolution behavior is quite different for the N implanted specimens compared with the as-polished specimen. This difference is discussed in more detail below.

### 5.2. Epoxy coated specimens

Cobalt ion release into the SBF from the as-polished (unimplanted) specimens coated with epoxy resin was below

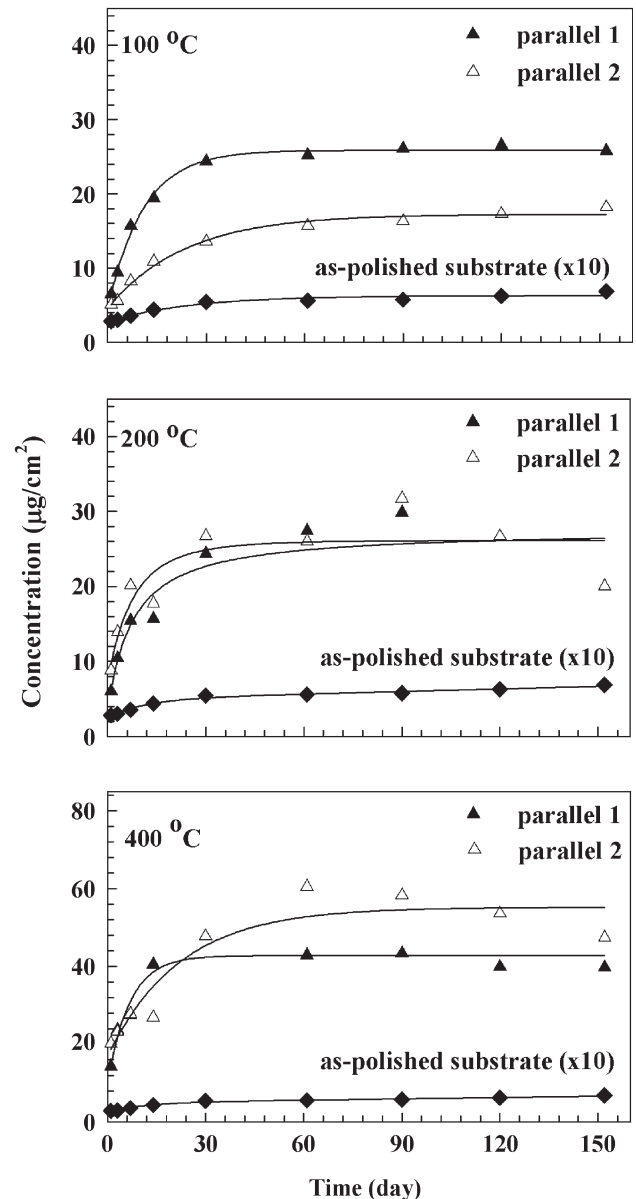


Fig. 5. The ETAAS data related to the concentration of the cobalt (Co) ions released into the simulated body fluid from the unimplanted CoCrMo alloy and the specimens nitrogen implanted at 100, 200, and 400 °C. Cobalt concentration released from the polished, unimplanted alloy has been multiplied by a factor of 10. (Note that the 'parallel 1' and 'parallel 2' specimens refer to the two immersion test pieces cut from the same nitrogen implanted disk specimen. Also note that in this figure the concentration values are given in units of  $\mu\text{g}/\text{cm}^2$ ; these values were obtained by dividing the concentration values in  $\mu\text{g}/\text{L}$  to the areas of the test specimens exposed to the SBF.)

the analytical detection limit of ETAAS (for Co prepared in SBF, the detection limit of the technique was 0.5 µg/L). The results for the epoxy coated polished specimen suggest that the epoxy coating does provide some form of physical barrier to the Co dissolution. This finding also indicates the ability of epoxy coating in preventing the dissolution of Co from the unimplanted sides of the N implanted immersion test specimens.

Chromium (Cr) and nickel (Ni) ion release into the SBF from the as-polished as well as the N implanted specimens were also found to be below the detection limit ETAAS (the detection limits for both Cr and Ni determinations in the SBF were ~0.5 µg/L). Similarly, molybdenum (Mo) ion release into the SBF from the as-polished and the N implanted specimens were analyzed by means of inductively coupled optical emission spectrometry (ICP-OES) and was found to be below the detection limit (~20 µg/L) of the technique.

## 6. SEM/EDX analysis after the immersion test

After the immersion test, the surface morphologies of the test specimens (as-polished CoCrMo alloy and nitrogen implanted specimens) were investigated by scanning electron microscopy as well as visually. In addition, qualitative and quantitative elemental analyses of the test specimen surfaces were carried out by energy dispersive X-ray (EDX) analysis. Before the SEM/EDX analysis, all the test specimens were washed with distilled water and dried at room temperature.

The visual inspection of the as-polished test specimen after the immersion test shows that about 50% of the surface appears to be covered with a white type of formation, which cannot be removed by repeated washing in water. There were no such formations on the surfaces of the N implanted test specimens examined visually after the immersion test. The SEM results after the immersion test for the as-polished substrate alloy is shown in Fig. 6. The SEM image shows the as-polished surface is coated with apparent mineral deposits, which appear slightly cracked but firmly adhered to the substrate. These results suggest that some precipitation took

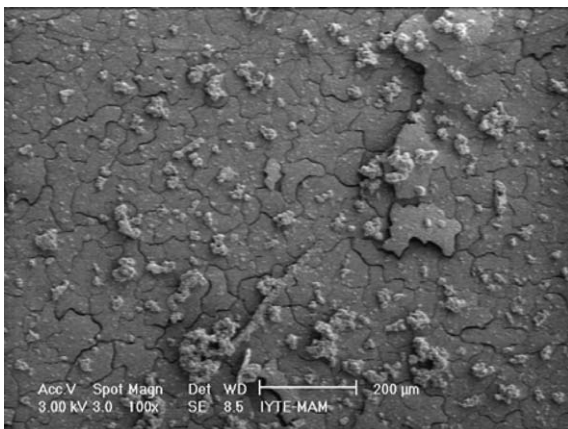


Fig. 6. The SEM results after the immersion test for the unimplanted alloy substrate.

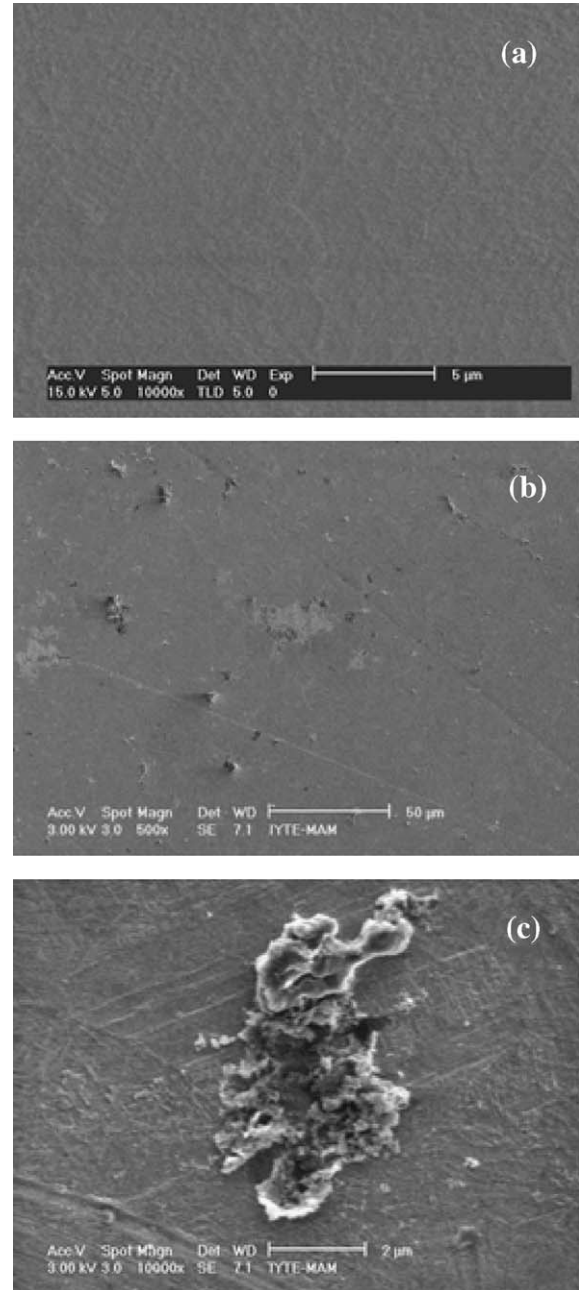


Fig. 7. The SEM results (a) before and (b, c) after the immersion test for the specimen nitrogen implanted at 100 °C.

place during the immersion test. The EDX analysis of these deposits (precipitates) reveals calcium and phosphorous peaks and indicate that the precipitates are highly enriched in Ca and P. This finding agrees quite well with a previous investigation (via XPS) that also showed calcium phosphate precipitation on CoCrMo alloy in Hank's solution and the culture medium [10].

The SEM results related to the surface morphologies of the N implanted test specimens after the immersion test are shown in Figs. 7–9. As can be seen from these figures, there was almost no precipitation taking place on the surfaces of the N implanted specimens during the immersion test. There were



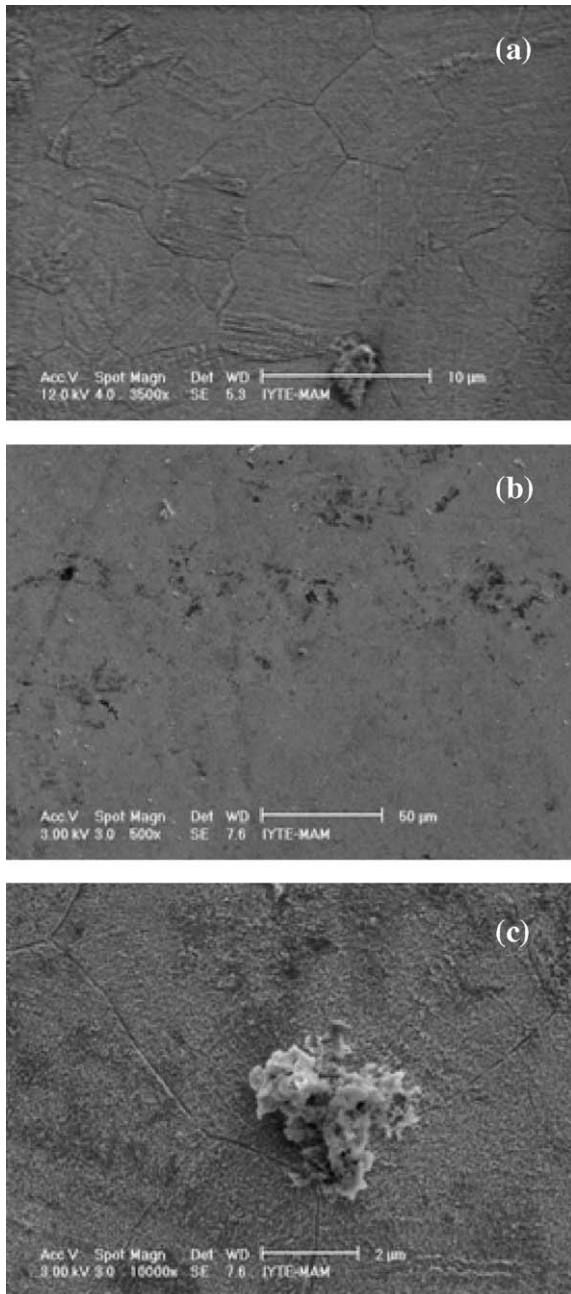


Fig. 8. The SEM results (a) before and (b, c) after the immersion test for the specimen nitrogen implanted at 200 °C.

only sparsely distributed regions (tiny white spots) where the precipitations (containing Ca and P) might have formed. However, by means of the EDX analysis the contents of these precipitations were not found to be rich in Ca and P. Note that in Figs. 8 and 9 the grain structure of the underlying substrate is revealed indicating that significant ion sputtering took place during the nitrogen ion implantation of the specimens. A natural consequence of the sputtering effect is an increase in the surface roughness for the N implanted samples, which, as discussed below, may be responsible in part for the higher Co ion dissolution into the simulated body fluid from the N implanted specimens compared to the as-polished substrate material.

## 7. Discussion

The results of the static immersion tests presented above suggest that the N implanted layers may not have any beneficial effect for reducing the Co ion levels released into the simulated body fluid. The results show a clear increase in Co ion release with the immersion time for the N implanted specimens compared to the as-polished (unimplanted) material. The reduced levels of Co ion release from the as-polished CoCrMo alloy might be attributed to the native oxide layer which serves as a barrier to the release of the Co ions from the substrate alloy. On the other hand, the increased levels of Co ion release from

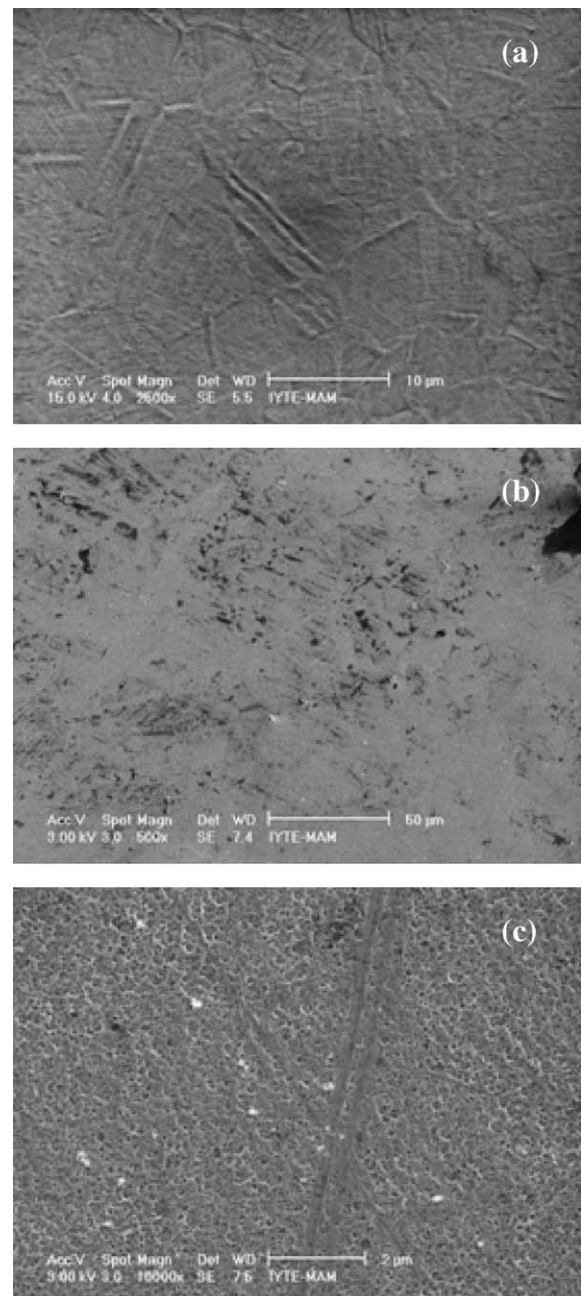


Fig. 9. The SEM results (a) before and (b, c) after the immersion test for the specimen implanted at 400 °C.

the N implanted specimens might be explained by the fact that the top N implanted layers do not inhibit the dissolution of cobalt ions in the implanted layers.

The results of the immersion tests also indicate that the specimen implanted at the substrate temperature of 400 °C has higher Co ion release levels than the specimens implanted at the substrate temperatures of 100 and 200 °C. As mentioned above, this difference may be attributed to the stability of the different N implanted layer phases formed on the CoCrMo alloy surface under the implantation conditions implemented here. In the  $\gamma_N$  phase (the N implanted layer phase for the specimen implanted at 400 °C), N atoms occupy the interstitial sites in the fcc lattice and they have a stronger bond with Cr than with Co (cobalt acts only as inert matrix element in the  $\gamma_N$  phase [21]). So, during in vitro exposure of the  $\gamma_N$  phase layer, it is easier for Co to be released from the  $\gamma_N$  phase. The limited dissolution of, on the other hand, Co ions from the specimens implanted at the substrate temperatures of 100 and 200 °C might be attributed to the  $(\text{Co,Cr,Mo})_{2+x}\text{N}$  nitride phase being more stable than the  $\gamma_N$  phase such that Co is not as available (i.e., due to the stronger bonds of metal-N than those of the  $\gamma_N$  phase).

As to why the Co ion release levels are all higher for the N implanted specimens compared to the as-polished CoCrMo alloy, a detailed analysis of the top surface layers (~ few nm) is necessary. The dissolution behavior of an implant material is affected by a number of surface controlled factors including the surface condition and nature of the oxide layer. The formation of this oxide layer may be controlled by the nature of the surface compounds, i.e., nitrides for the implanted specimens versus a metallic alloy for the as-polished specimen.

The surface condition also involves the smoothness of the material's (CoCrMo alloy) surface, i.e., roughness. The surface roughness values ( $R_a$ 's) were measured by AFM and are listed in Table 1. They clearly indicate that surface roughness is increased by nitrogen ion implantation treatment. The mean roughness for the as-polished specimen was found to be ~ 2 nm, while the roughness values for the N implanted specimens were about 6, 12, and 8 nm for the 100, 200 and 400 °C implanted samples, respectively. Also, the SEM images (Figs. 8 and 9) clearly indicate much rougher surfaces for the N implanted specimens compared to the as-polished substrate surface. As a consequence, a greater surface area is available for metal ion release from the N implanted surfaces via oxide dissolution or micro-scale corrosion reactions. A recent study [22] investigating the effect of surface roughening on metal ion release found higher levels of aluminum ion release from Ti–6Al–4V titanium alloy femoral stems that were grit blasted compared to the polished Ti–6Al–4V stems. The grit blasted specimens had a surface roughness of 4.0  $\mu\text{m}$ , while the polished stems had a roughness of about 1.0  $\mu\text{m}$ . In this study, before the immersion test, the polished and grit blasted stems were treated with a surface-oxide-forming condition (aging the stems in boiling de-ionized water for a certain time).

In addition to the phase stability and surface roughness arguments given to explain higher Co ion release levels from the N implanted surfaces, a detailed analysis of oxide layer(s) formed on the N implanted surfaces both before and after the

immersion tests seems to be necessary. There is no conclusive evidence on the formation of oxide film(s) based on the experimental results obtained here. Although an oxide layer might have formed during the nitrogen implantation of the as-polished CoCrMo alloy materials, it is likely that a thin oxide layer would form on the surfaces of the N implanted specimens in air after the implantation. In fact, a plasma immersion ion implantation study of 316 SS gives evidence of oxide layer formation on the N implanted surface [20].

The results of the static immersion tests represented in Fig. 5 clearly indicate different Co ion dissolution behavior for the N implanted specimens in comparison with the as-polished (unimplanted) specimen suggesting different dissolution mechanism(s) for the N implanted and unimplanted specimens. As can be seen from this figure, the Co ion release is quite steep for the N implanted specimens compared to the as-polished material. This observation suggests there are significant ion release processes occurring upon immersion of the N implanted specimens into the SBF, while the dissolution process is somehow inhibited for the as-polished specimen immediately upon immersion. As can be seen from this figure, the ion release rate (determined by the slope of the ion release versus the immersion time curve) is initially quite high for the N implanted specimens compared to the as-polished material. The higher ion release rate for the N implanted specimens suggests a higher rate constant. The general shape of ETAAS data in Fig. 5 (steep rise followed by saturation) suggest a diffusion or transport controlled dissolution process [22].

Although the ETAAS results indicate higher cobalt ion dissolution from the N implanted surfaces, the ion levels remain below any toxic levels and nitrogen ion implantation can still be used to enhance the corrosion resistance for orthopedic alloys since the cross-sectional SEM results indicate that the electrochemical etch used strongly attacks the substrate phase ( $\gamma$ ), while the N implanted layer phase ( $\gamma_N$ ) is not attacked by the same etch, suggesting an enhanced corrosion resistance for the implanted layer.

## 8. Conclusions

In this research, the effectiveness of nitrogen ion implanted layers on CoCrMo alloy in preventing metal ion release into a simulated body fluid was investigated. The experimental results show that the N implanted layers are not as effective and efficient in preventing and/or reducing metal ion dissolution into the SBF as the as-polished substrate material.

The XRD results clearly show that the N ion beam conditions, namely ion beam energy of 60 keV, a high dose of  $1.9 \times 10^{18}$  ions/cm<sup>2</sup> for an implantation time of 30 min, lead to a metastable, fee high N concentration phase ( $\gamma_N$ ) in mainly fcc CoCrMo alloy for a substrate temperature of 400 °C, while the lower implantation temperatures of 100 and 200 °C result in a nitride phase,  $(\text{Co,Cr,Mo})_{2+x}\text{N}$ . The SEM analysis results reveal quite clearly the uniform nature of the  $\gamma_N$  layers with a reasonably well defined interface between the  $\gamma_N$  layer and the substrate, suggesting uniform N contents with uniform layer thicknesses. Based on the SEM results, the average  $\gamma_N$  layer

thickness was found to be 450 nm, while the  $(\text{Co,Cr,Mo})_{2+x}\text{N}$  nitride layer thickness was found to have a range from 150 to 200 nm. The cross-sectional SEM results also show that the electrochemical etch used strongly attacks the substrate phase ( $\gamma$ ), while the N implanted layer phase,  $\gamma_{\text{N}}$ , is not attacked by the same etch, suggesting an enhanced corrosion resistance for the substrate alloy as a result of N ion implantation into this alloy.

Metal ion release into the body fluid from the as-polished and N ion implanted specimens were analyzed by ETAAS and ICP-OES. The ETAAS results show that in vitro exposure of the N implanted surfaces results in higher levels of cobalt ion release into the simulated body fluid than the as-polished substrate alloy. The higher Co dissolution from the N implanted specimens was attributed to the nature of the implanted layer phases. It was explained that during in vitro exposure of the  $\gamma_{\text{N}}$  phase layer, it is easier for Co to be released from the  $\gamma_{\text{N}}$  phase compared to the  $(\text{Co,Cr,Mo})_{2+x}\text{N}$  phase. The lower levels of Co ion release from the specimens implanted at 100 and 200 °C was attributed to the nitride phase  $(\text{Co,Cr,Mo})_{2+x}\text{N}$  being more stable compared to the  $\gamma_{\text{N}}$  phase. In addition to the phase stability concept, the higher cobalt ion release levels from the N implanted specimens may be enhanced by the rougher surfaces associated with the N implanted specimens compared to the relatively smooth surface of the as-polished substrate material.

The lower levels of Co ion release from the as-polished CoCrMo alloy as compared to the N implanted specimens was attributed to the native oxide layer and rather smooth surface of the polished specimen. The SEM/EDX investigation of the N implanted and as-polished specimens after the static immersion test clearly indicated calcium phosphate formation on the as-polished CoCrMo alloy, indicating a degree of bioactivity of the as-polished surface, which is absent in the N implanted surface.

## Acknowledgments

We would like to thank Prof. Paul J. Wilbur of Colorado State University for performing the nitrogen ion implantation. We acknowledge the contributory discussions of Prof. Şebnem Harsa. We are in debt to Sinan Yilmaz and Oya Altungöz for their help with the ETAAS and ICP-OES analyses. The authors would also like to thank HIPOKRAT A. Ş. for providing medical grade CoCrMo materials for this study. This project was partially funded by Izmir Institute of Technology through grant IYTE 2003/14.

## References

- [1] M. Long, H.J. Rack, *Biomaterials* 19 (1998) 1621.
- [2] K.S. Katti, *Colloids Surf., B Biointerfaces* 39 (2004) 133.
- [3] V. Biehl, J. Breme, *Mat. -wiss. U. Werkstofftech.* 32 (2001) 137.
- [4] I. Milosev, H.H. Strehblow, *Electrochim. Acta* 48 (2003) 2767.
- [5] Y. Okazaki, E. Gotoh, *Biomaterials* 26 (2005) 11.
- [6] M.G. Shettlemore, K.J. Bundy, *Biomaterials* 22 (2001) 2211.
- [7] T. Hanawa, S. Hiromoto, K. Asami, *Appl. Surf. Sci.* 183 (2001) 68.
- [8] J.R. Goldberg, J.L. Gilbert, *Biomaterials* 25 (2004) 851.
- [9] A. Wisbey, P.J. Gregson, M. Tuke, *Biomaterials* 8 (1987) 477.
- [10] S.K. Yen, M.J. Guo, H.Z. Zan, *Biomaterials* 22 (2001) 125.
- [11] C.A. Straede, N.J. Mikkelsen, *Surf. Coat. Technol.* 84 (1996) 567.
- [12] R. Leuteneker, G. Wagner, et al., *Mater. Sci. Eng., A* 115 (1989) 229.
- [13] F.Z. Cui, Z.S. Luo, *Surf. Coat. Technol.* 112 (1999) 278.
- [14] S. Mandl, B. Rauschenbach, *Surf. Coat. Technol.* 156 (2002) 276.
- [15] D. Ikeda, M. Ogawa, Y. Hara, Y. Nishimura, O. Odusanya, K. Azuma, S. Matsuda, M. Yatsuzuka, A. Murakami, *Surf. Coat. Technol.* 156 (2002) 301.
- [16] B.R. Lanning, R. Wei, *Surf. Coat. Technol.* 186 (2004) 314.
- [17] O. Öztürk, D.L. Williamson, *J. Appl. Phys.* 77 (1995) 3839.
- [18] P.J. Wilbur, L.O. Daniels, *Vacuum* 36 (1986) 5.
- [19] B.D. Cullity, *Elements of X-ray Diffraction*, Addison Wesley Publishing Company, Inc., 1978, p. 138.
- [20] S. Mukherjee, P.M. Raole, P.I. John, *Surf. Coat. Technol.* 157 (2002) 111.
- [21] T. Kilner, A.J. Dempsey, R.M. Pilliar, G.C. Weatherly, *J. Mater. Sci.* 22 (1987) 565.
- [22] M. Browne, P.J. Gregson, *Biomaterials* 21 (2000) 385.